

BURNUPS: TRANSURANUS VERSES FREY

H. Wallin, PSI Sci. Report 2001, vol IV

In this article, fuel rod behaviour in reactivity-initiated accidents is discussed, especially the fuel rod failure mechanisms that are encountered at high burnups. The applicability of the computer codes TRANSURANUS (TU)* and FREY to Reactivity Initiated Accidents (RIA) modelling at high burnups is assessed, and some results of a comparison between RIA simulations using the code packages TU and FREY are presented.

1 INTRODUCTION

A special case of the class of *Reactivity-Initiated Accidents (RIAs)* is the *Control Rod Ejection Accident (REA)*¹. The ejection of a control rod from a reactor core causes a sudden increase in reactivity, and subsequent power pulse. Due to the very short time in which energy is deposited in the fuel, the fuel heats up nearly adiabatically and, if the power burst is sufficiently energetic and rapid, it may damage, or even destroy, the fuel rod.

At PSI, modelling of fuel rod behaviour under accident conditions—either RIA and Loss-of-Coolant Accident (LOCA) conditions—is performed within the STARS project.

The code TRANSURANUS (TU) has been traditionally used at PSI to calculate the behaviour of pellet rods under normal conditions [1]. Although the code has not been developed explicitly for accident calculations, it can be used for RIA and LOCA events in cases where its limitations in modelling strategy are insignificant. Additionally, PSI has purchased the code FREY (Fuel Rod Evaluation System), which was specifically developed for transient and accident conditions, [2].

A comparison between TU and FREY has been undertaken in order to evaluate the particular advantages and disadvantages of the two code systems. The behaviour of a UO₂ fuel rod has been calculated using both codes for the following "test case":

- RIA under typical PWR conditions at zero reactor power;
- a rod average burnup of 47.7 MWd/kgU;
- reactivity insertion of 1.75 \$; and
- peak enthalpy rise of $\Delta H_{\max}=51$ cal/g (corresponding to $H_{\max}=70$ cal/g).

The base irradiation to 47.7 MWd/kgU was first calculated using TU, and the output then used as input to the RIA calculations. The chosen test case was specifically defined for this code comparison exercise, and might not represent a realistic case in all aspects.

2 FUEL ROD BEHAVIOUR IN RIA

An overview of rod thermal behaviour during RIAs is given below, based on a simulation using FREY.

¹ Although REA is the more exact term denoting a rod ejection accident, RIA is the more widely known abbreviation, and is frequently used interchangeably with REA.

Radial profile of temperature

Figure 1 shows the temperatures in Axial Slice 11, as calculated by FREY, for 10 radial positions (7 nodes in the fuel, 3 in the cladding), for a few selected time steps. At the beginning of the RIA, the temperature is highest at the fuel rim. As the fuel heats up almost adiabatically, the radial temperature profile has roughly the shape of the radial power profile: i.e. temperature is highest in the rim area and decreases gradually towards the fuel centre (Fig. 1).

After peak power occurs at 0.226 s, the temperature profile changes as the heat from the rim is both conducted inwards towards the centre, and outwards to the cladding and the coolant. Power continues to be generated in the fuel (after 1 s it is still 25 kW/m), and as a result the radial temperature profile shifts towards the normal parabolic profile characteristic of steady-state operation.

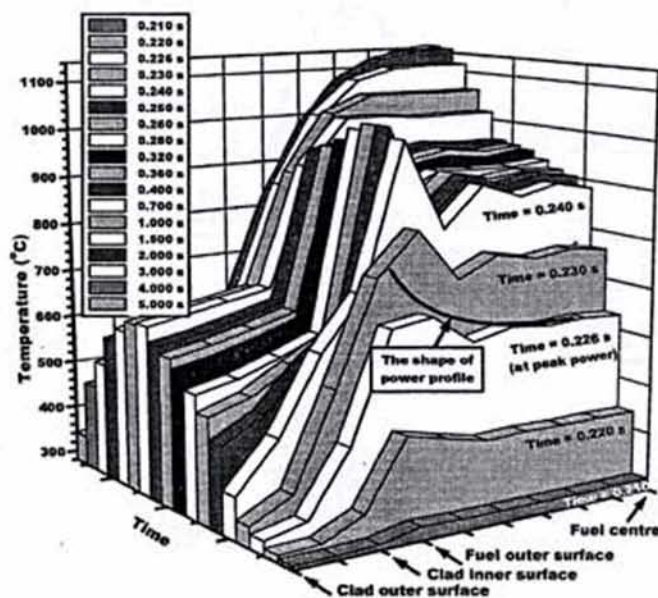


Fig. 1: Temperatures in 10 radial nodes at selected time steps (Axial Slice 11, FREY calculation).

Axial profile of central temperature

Figure 2 shows the axial profile of the fuel central temperature as a function of time. The temperatures continue to rise following the power peak (line A), and still rise after the power has decreased to below 1% of the maximum power level (line B).

Axial profile of fuel outer temperature

In a RIA at high burnup, the temperature at the pellet rim is critical due to the large potential for gaseous

swelling, both in High Burnup Structure (HBS) and in the unstructured fuel. Figure 3 shows the axial profile of the fuel outer temperature as a function of time.

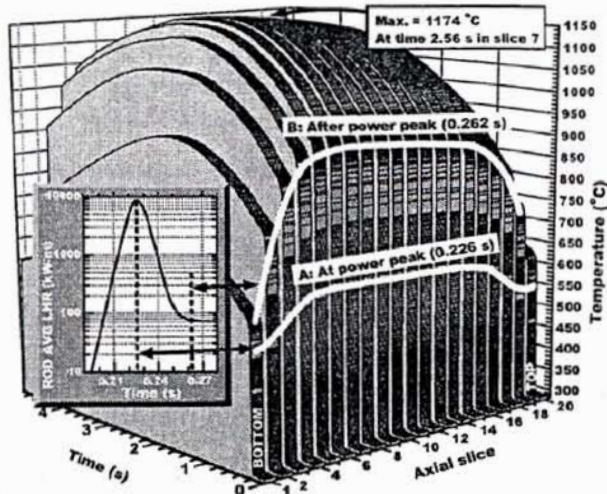


Fig. 2: Axial profile of fuel central temperature vs. time (FREY)

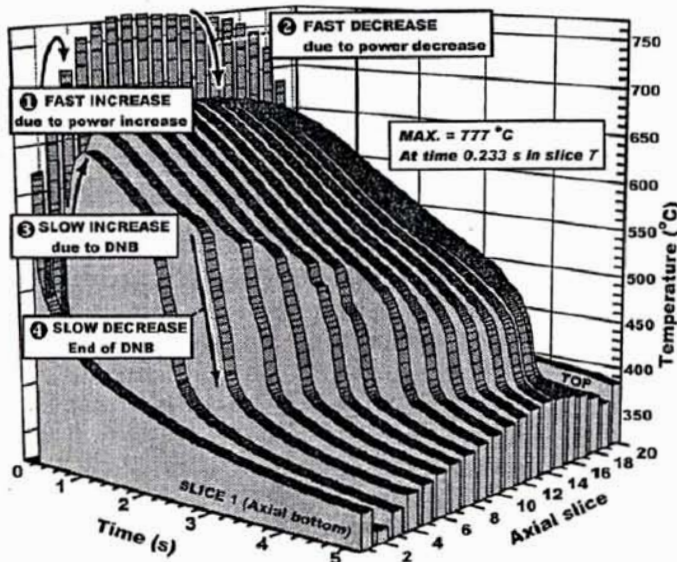


Fig. 3: Axial profile of fuel outer temperature vs. time (FREY)

Fuel outer surface temperatures exhibit four phases: (i) rapid increase, (ii) rapid decrease, (iii) a slower increase, and (iv) a still slower decrease. To describe the origins of these four phases, the principal phenomena having an effect on the fuel outer temperature have been displayed in Fig. 4.

- The power increase is initiated at 0.200 s and peaks at 0.226 s. Up to the time of maximum power, the temperatures both in the centre and at the rim increase nearly at the same rate. The increase in gap conductivity due to the gap closure (at 0.220 s) had nearly no effect on the fuel temperature increase rate.
- After the power peak, fuel outer temperatures

and (further) to the coolant. In contrast to this, the central temperatures continue to rise due to the continued heat generation (although at a much lower level), and the poor thermal conductivity of UO_2 , which prevents rapid heat transfer from the fuel centre.

- The fuel outer temperature increased slowly due to the onset of DNB² at 0.24 s (Axial Slices 3 – 19).
- After the end of the DNB phenomenon (starting from Axial Slice 3 and proceeding towards the upper end of the rod), the fuel outer temperature decreases slowly.

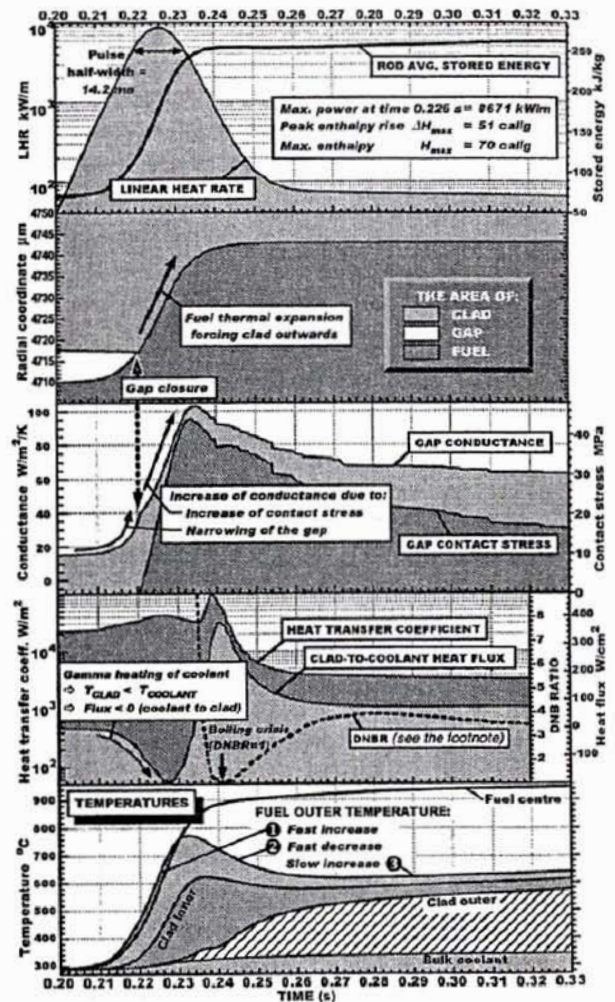


Fig. 4: Phenomena affecting fuel temperatures (FREY).

- Departure from Nucleate Boiling (DNB). Denotes a boiling crisis in Pressurised Water Reactors, and occurs if the clad temperature exceeds a certain value at which the highly effective heat-transfer mechanism of nucleate boiling changes to the highly inefficient mechanism of film boiling, in which clad/coolant heat transfer is degraded by the presence of an "isolating" vapour film on the clad surface.

Critical Heat Flux (CHF) is the value of the heat flux at which the boiling crisis occurs; and the DNB ratio (DNBR)

3.1 The role of high burnup structure

At present, the most investigated single item of UO_2 fuel is the formation of the *High Burnup Structure (HBS)*, and especially the effect it has on pin behaviour during an RIA. Namely:

- with increasing burnup, the decrease of the energy deposition required for rod failure (for which HBS is, together with the structural changes of the cladding, the most important single factor); and
- the effect on the fuel thermal conductivity.

HBS can be characterised by three typical features:

- 1) subdivision of the original fuel grains into ~10 000 new grains, with diameters of 0.1 - 0.3 μm ("cauliflower structure");
- 2) depletion of intra-granular fission gas; and
- 3) formation of large faceted pores (\varnothing ~1 μm), which contain most of the fission gas originally in the fuel, and which increase the fuel porosity by up to 20%.

HBS is always formed as a consequence of irradiation to high burnups at low temperatures (below 1100-1200°C). The potential candidates that could cause grain subdivision are listed:

- 1) Overpressurisation of the fission gas bubbles. To relieve gas pressure, the bubbles must increase their volume. However, this is possible only by absorption of vacancies. Due to the low mobility of vacancies at low temperatures, insufficient quantities of vacancies arrive at the bubble, and bubble growth is prevented.
- 2) Lattice stress caused by fission products.
- 3) Accumulation of irradiation defects.

In HBS, gas pressure in the pores and in the bubbles is far higher than in the inner part of the fuel. For example, in intra-granular nm-sized bubbles, the gas pressure can be as high as 1.2 GPa, which is the pressure at which Xe is near or at a solidus state. The pressure in large, μm -size pores is lower, but still of the order of 30-40MPa. If the temperature is increased, the highly pressurised fission gas has a considerable potential to cause fuel swelling. Out-of-pile annealing of samples with burnups of 80 MWd/kgM have shown immediate and "explosive" fragmentation of the sample, even at temperatures of 700°C.

The formation of HBS starts when the local, microscopic burnup reaches a threshold of 60 - 75 GWd/tM, at which the first isolated spots of HBS, surrounded by unrestructured fuel, are formed. At a local burnup of ~120 GWd/tM, 100% of the fuel has been transformed into HBS form.³

³ At the pellet rim, a local burnup of 70 GWd/tM is reached at a cross-sectional average burnup of ~40 GWd/tM (for standard LWR conditions and enrichment; i.e. ~4%).

3.2 Fuel swelling during RIA

In RIA, a rapid fuel temperature increase causes an increase in fuel volume due to [3, 5]:

- 1) thermal expansion of the fuel;
- 2) gaseous swelling of the fuel due to the thermal expansion of the fission gas in
 - a) nm-sized grain boundary bubbles,
 - b) nm-sized intra-granular bubbles, and
 - c) μm -sized pores (as-fabricated or pores in HBS);
- 3) growth of the existing bubbles, and formation of new ones (though it is uncertain if the short temperature pulse in RIA is long enough for thermal diffusion to bring gas into the bubbles); and
- 4) coalescence of fission gas bubbles, since after coalescence the gas occupies a larger volume, even if the amount of gas remains the same⁴.

Above the cross-sectional-averaged burnup of 40 MWd/kgU, HBS starts to form, and some new mechanisms take place, roughly in the following order (see Fig. 5):

- 5) rapid growth of the overpressurised μm -sized pores and nm-sized bubbles, due to the increased mobility of vacancies and fission gas;
- 6) fuel grain boundary separation causing fuel fragmentation⁵;
- 7) cladding deformation, due to thermal expansion of the fuel and gaseous swelling; and
- 8) in the last phase, burst release of the gas to the rod free volume. (Burst release decreases gaseous swelling, and relieves the stress on the cladding. In the later phase of the RIA, burst release increases somewhat the rod inner gas pressure, but the extra load on the cladding, due to this pressure increase is smaller than the load the gas would have caused by remaining in the fuel.)

⁴ Larger bubbles have lower gas pressure because of the smaller surface tension (or smaller surface curvature). For example if N bubbles coalesce to form N/2 new bubbles, the volume occupied by the gas increases by 40%; i.e., gaseous swelling of fuel increases by 40% [7].

⁵ The equivalent term is "grain boundary decohesion", which occurs in HBS, in the transition zone, or in unrestructured fuel if the gas pressure in grain boundary bubbles exceeds the fuel fracture stress.

RIA. Consequently, fuel rods with identical burnups can behave differently during the RIA, due to the factors listed below.

- There is the possibility of enhanced cladding corrosion and spallation due to coolant conditions, water chemistry or cladding material type.
- A Gd rod accumulates burnup at the beginning of the irradiation relatively slowly, but its cladding is exposed to the same corrosion and irradiation damage as a standard UO₂ rod.
- If the rod has been irradiated at high temperature, it has experienced high fission gas release, and less gas is left in the fuel to cause swelling during the RIA.
- Compressive loads in the fuel caused by PCMI (due to fuel swelling and clad creep-down) reduce grain boundary bubble sizes. Consequently, bubble interlinkage and fission gas release is delayed and more gas accumulated at grain boundaries, which can cause high fuel swelling and gas release during the RIA.

Therefore, just presenting $\Delta H_{failure}$ against fuel burnup must be seen merely as a way to show the range at which the RIA tests have been performed, and not as an indisputable dependence on burnup. For rod failure predictions, a better alternative might be to plot $\Delta H_{failure}$ as a 3-dimensional surface ($\Delta H_{failure}$ as the z-coordinate) against:

- burnup (x-coordinate), which captures the change in fuel material properties with increasing burnup, the formation of HBS, fission gas generation (though not its distribution), etc.; and
- cladding ductility (y-coordinate), which incorporates the effect of hydrides, spallation, etc.

4.1 The NRC acceptance criteria for RIA

The US NRC⁷ has set down the guiding principles determining fuel rod damage limits in the General Design Criterion 28 (GDC-28), which states that RIA should neither:

- damage the reactor pressure boundary beyond limited local yielding; nor
- significantly impair the coolability of the core.

According to Regulatory Guide 1.77, GDC-28 is considered to be satisfied if the peak cross-sectional averaged enthalpy of the fuel does not exceed 280 cal/g. This limit was thought to prevent:

- fuel dispersal to the coolant, which could cause pressure waves that could threaten the reactor pressure boundary; and
- loss-of-coolability of the core due to cladding failure, leading to a substantial reduction in the coolant flow channel area due to fuel rod deformation and dispersed fuel and cladding

material. (Cladding failure is acceptable if it can be shown that core coolability is maintained.)

At the time when the enthalpy limit of 280 cal/g was set, data was available (mainly from low burnup situations), and only four fuel tests related to RIA issues had been performed above 6 GWd/tM. Since then, RIA tests have been performed beyond 60 GWd/tM. Some of them have shown fuel failures at low energy depositions, which has called into question the adequacy of the enthalpy limit of 280 cal/g.

5 APPLICABILITY OF TU AND FREY TO RIA AT HIGH BURNUPS

5.1 Verification, validation, qualification

In general, several different methods are available for assessing computer codes. Slightly simplifying, the division can be set out as described below.

- **Verification:** the most limited process, which checks that the software implementation of the model is done correctly, that it behaves qualitatively as expected, etc.
- **Validation:** checking that, for the intended task, the models are used only in their range of validity.
- **Qualification:** the broadest term, which goes beyond verification and validation. Put simply, the task is to show that the code is adequate for the intended task. As the codes have a variety of different options, and, as a large part of the modelling is performed by correctly defining the code input, the ultimate responsibility in qualification rests with the code user.

It is not sufficient that the numerical simulation can reproduce overall rod behaviour in an irradiation test. It is also necessary to show that this has been achieved by:

- modelling exactly those phenomena that are considered the most important; and
- that the relative importance of the phenomena in the code calculation corresponds to what is the "widely-held opinion"⁸.

The present comparison between the codes TU and FREY is an example of the code-to-code comparisons useful to map differences between the codes, but are really nothing more than that. It does not validate or qualify either of them.

5.2 High burnup issues in RIA and their implementation in TU and FREY

The validity of high burnup RIA calculations depends on:

- the applicability of the models to high burnup situations; and
- whether the phenomenon the model is intended to represent has an importance in RIA.

7 U.S. Nuclear Regulatory Commission

8 "Widely-held opinion" is best documented in the NRC's "Phenomena Identification and Ranking Tables" (PIRT), which identify the most important phenomena, and give their relative ranking in different transient and accident sequences.

Table 1: FREY vs. TRANSURANUS—Implementation of high-burnup phenomena that have an importance in RIA.

Phenomenon	Validated models in FREY	Validated models in TRANSURANUS
Decrease in clad ductility due to oxidation, hydriding, spallation, radial distribution of hydrides, and irradiation damage.	Clad mechanical properties & clad damage: • models are based on data at low burnups, • models do not depend on hydrogen concentration.	Clad mechanical properties & clad damage: • models are based on data at low burnups, • models do not depend on hydrogen concentration.
Gaseous fuel swelling in fast transients (including grain boundary separation).	Not implemented.	Not implemented.
Fission gas burst release (transient conditions).	Simple explicit correlation depending only on temperature. Questionable if model can be used at high burnup. Not applicable to HBS.	Not implemented.
Radial power profile at high burnup.	Implemented, but underpredicts power in rim.	Validated model implemented.
Fuel thermal conductivity.	The default low burnup model can be changed to a high burnup model by the user.	Implemented. Porosity in HBS taken into account.

Table 1 shows the high-burnup phenomena of importance during the RIA, and the status of their implementation in FREY and TU (implemented models are shaded⁹). Some of these issues are discussed in more detail later in this Section.

As TU and FREY are not applicable to high burnup calculations, the codes cannot be used as such to calculate the energy deposition leading to clad failure at high burnup. The problem cannot be solved by adding some explicit correlations to the codes. For example, gaseous swelling can be calculated only with a code having a mechanistic fission gas model capable of "keeping track" of the fission gas during the whole base irradiation; i.e. modelling the distribution of the fission gas and the bubble sizes.

If an applicable code is not available for high burnups, RIA calculations can be supplemented with a rough estimate of the gaseous swelling (or of its insignificance). This could be performed with the code SPHERE-3, for example, which has a mechanistic fission gas model. SPHERE-3 had been originally developed at PSI to calculate the fuel behaviour of sphere-pac fuel, but recently the code has been modified for pellet fuel.

5.3 Clad material properties in FREY and TU

TU has only very basic correlations for the LWR-clad material. Only Zircaloy and Zr1Nb cladding (used in VVERs) models have been implemented. The correlations for rupture strain and yield stress consist of fixed values, without a burnup dependence. Apart from the basic correlations, the user can implement

⁹ Phenomena like fuel grain growth, fuel restructuring, etc. are affected by burnup, but they occur only during the base irradiation prior to the RIA, not during the short time of the RIA itself. Strictly, correct modelling of RIA in transient codes is therefore not important. However, they do determine the initial conditions for the RIA calculations, and their correct modelling in base irradiation is important for

his own cladding correlations into the code. This applies also to FREY.

6 OUTLINE OF THE CODE COMPARISON

6.1 Validity of the code calculations in the selected test case

The codes TU and FREY were compared by calculating an RIA under characteristic PWR conditions. The RIA case corresponds to a typical 1.75\$ rod ejection accident at hot-zero power, calculated with 3-dimensional kinetics.

The burnups are (Fig. 6):

- rod average: 47.7 MWd/kgU
- max. cross-sectional avg. (Slice 7): 54.5 MWd/kgU
- max in the centre (Slice 7): 48.0 MWd/kgU
- max in the rim (Slice 7) : 119 MWd/kgU

HBS is found in all axial slices, except in Slices 1 and 20. As both FREY and TU do not have models for most high-burnup phenomena, the present work can not be seen as an attempt to perform a proper RIA analysis, but merely as a comparison of the codes. The main focus was on temperature levels, stresses in the clad, radial deformation, and the radial power distribution.

6.2 Common thermal boundary conditions

Both FREY and TU have a flow channel model, which calculates thermal boundary conditions for fuel pin analysis (rod-to-coolant heat transfer coefficients and coolant temperatures).

The flow channel model of TU cannot handle extreme accident conditions and, for example, the present version is not capable of modelling DNB. The coolant channel model in FREY also has its limitations, and is applicable only to pre-DNB heat transfer conditions.

Therefore, in a proper RIA analysis, both codes require thermal boundary conditions to be provided by an external thermal-hydraulics code. For this reason, the flow-channel models were excluded from

outer temperatures during the first 100 s, then using these values as boundary conditions for the TU calculation.

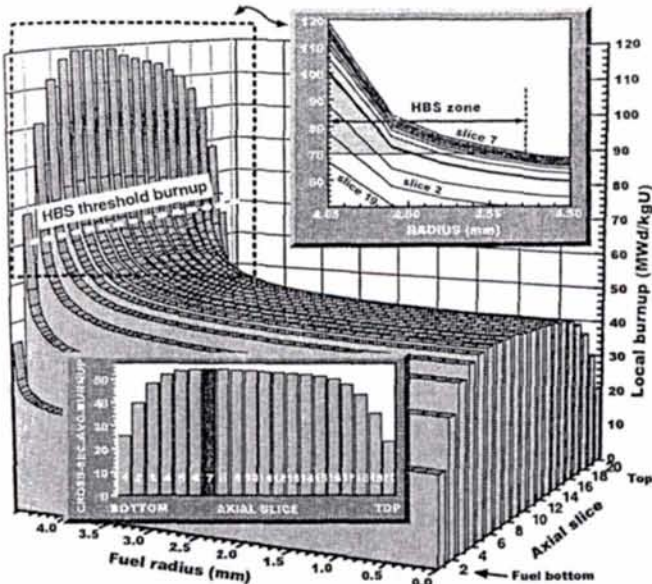


Fig. 6: Local and cross-sectional average burnup.

7 INPUT DATA FOR CODE COMPARISON

7.1 Input data for TU (base irradiation and RIA)

The input data for TU is listed in Table 2. Modelling was performed using 20 axial fuel slices. In the radial direction, the fuel was divided into 16 coarse zones, and the clad into 2 coarse zones. These coarse zones were further subdivided, typically with 3-10 mesh points per zone.

Table 2: Pin, fuel and clad data in TU calculation.

Pin Data		
Fuel column length	mm	3 023.0
Upper plenum length	mm	145.8
Fill gas (He) pressure at fabr.	MPa	2.3 (at 25°C)
Fuel Data (UO ₂)		
Outer pellet radius	mm	4.6455
Dish volume/Pellet volume	—	0.0223
Enrichment (U ²³⁵)	%	4.3
Cladding (Zircaloy) Data		
Inner/outer radius	mm	4.743 / 5.360
Base irradiation (5 cycles):		
Coolant pressure	MPa	15.75
Coolant temperature	°C	286–315
Rod average LHR (kW/m)		14/15.5/23/22/20
Time per cycle (h)		7500/7500/7500/7499/7200

7.2 Input data for FREY (RIA)

Most of the material properties and calculational models in FREY are taken from the MATPRO handbook [6]. The models for fuel thermal conductivity, porosity correction and degradation of conductivity with increasing burnup were changed to

the same models as used in the TU calculation. After base irradiation, the thickness of the clad oxide layer was 84 μm.

8 COMPARISON OF TU AND FREY RESULTS

8.1 Rod deformation calculated using FREY

Figure 7a shows the rod dimensions after base irradiation under cold conditions (TU); as-fabricated dimensions are shown for comparison. During base irradiation, the as-fabricated radial gap of 97.5 μm had decreased to about 10 μm (cold gap) due to fuel swelling and cladding creep-down.

Figure 7b compares the rod dimensions calculated by TU and FREY at the time of maximum radial fuel deformation (1.000 s for TU and 1.601 s for FREY). The rod dimensions in hot-stand-by conditions just prior to the RIA are shown for comparison.

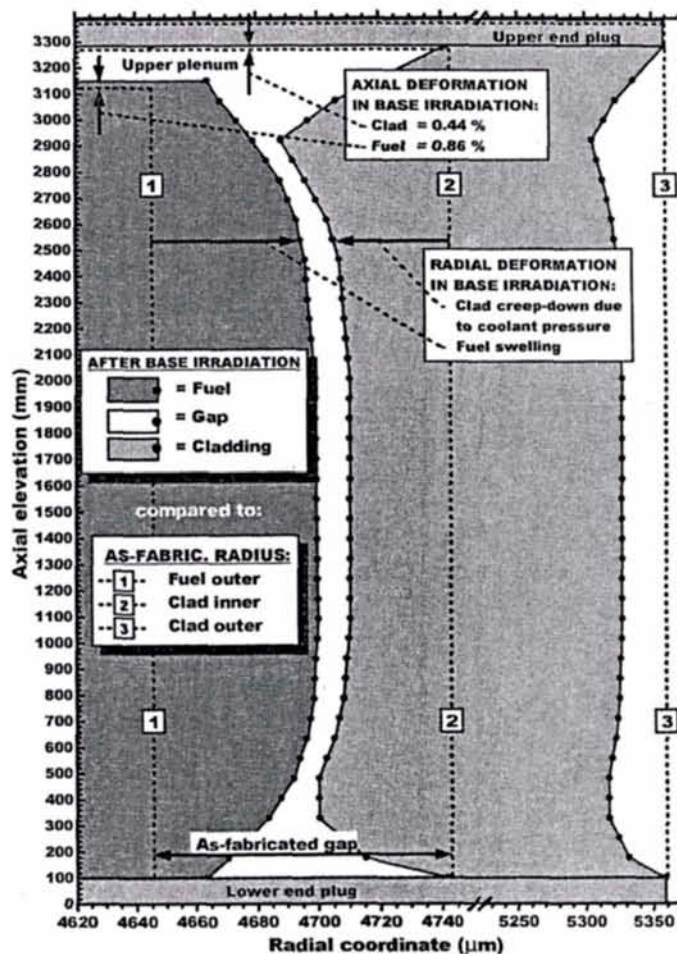


Fig. 7a: Dimensions (cold) after base irradiation (FREY)

8.2 Comparison of fuel outer radius

Figure 9 compares the fuel and clad radii calculated with TU and FREY. Rapid thermal expansion of the fuel causes almost immediate gap closure, after which the clad is forced outwards.

¹⁰ Both codes provide a user option to change these correlations. In this exercise, the same correlations were chosen for both codes.

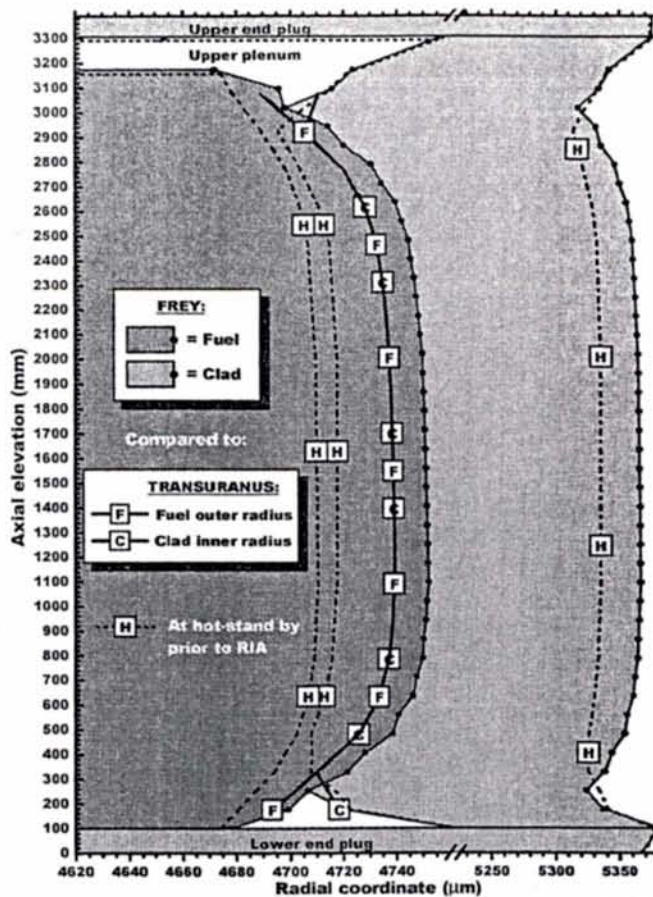


Fig. 7b: Maximum radial fuel deformation (FREY vs. TU)

FREY calculated 7–10 μm greater increase in fuel outer radius during the RIA. This difference was nearly the same in all axial slices. Edge temperatures were the same for both the TU and FREY calculations, but FREY calculated 40–50°C higher central temperatures. This would cause ~3 μm greater thermal expansion in the hottest axial slice, not enough to explain the difference of 7–10 μm .

8.3 Comparison of gap thermal conductance

As expected, at the beginning of the RIA, the higher fuel radial expansion in the FREY calculation leads to both higher contact pressure and better gap conductivity (Fig. 9). After the initial phase, the contact pressure is seen to decrease faster in FREY than in TU, and FREY gives ~30% lower gap conductance than TU during the rest of the calculation.

8.4 Comparison of radial power distribution

At the beginning of irradiation, fissile isotopes consist only of U-235, with no radial variation. During the irradiation, fissile plutonium builds up at the edge due to the epithermal neutron capture in U-238. With increasing burnup, fissile plutonium concentration

sectional average of ~1%, and to a local value of ~3% at the pellet rim.

As the fission rate in the fuel is directly proportional to the concentration of fissile isotopes, the fission rate at the pellet rim is typically 200%–350% higher than in the pellet inner area at high burnups (in LWR conditions and with standard enrichments).

FREY uses the RADAR model for calculating the radial distribution of fissile isotopes and power, while TU uses the TUBRNP model (the RADAR model is also available in TU, but is a newer version than the one in FREY). Due to the different models, and due to the coarser radial nodalisation in FREY, the radial power profile in FREY is flatter than in TU, as can be seen in Fig. 8. Consequently, at the same power, FREY calculates less heat production at the rim, where the potential for gaseous swelling in RIA is highest.

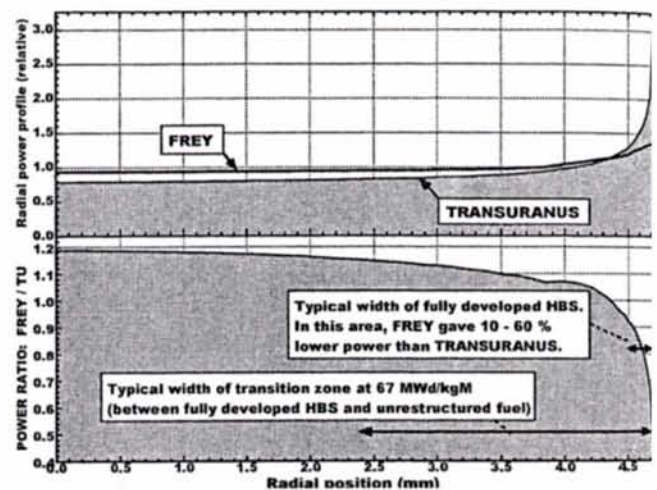


Fig. 8: Radial power profile (FREY vs. TU)

8.5 Comparison of temperature

Clad outer temperatures were the same in the TU and FREY calculations simply because TU used the clad outer temperatures calculated by FREY as a boundary condition. The clad inner temperatures and fuel outer temperatures were also nearly identical.

FREY gave 40°C–50°C higher fuel central temperatures than TU (Fig. 9), this in spite of the same correlation for fuel thermal conductivity and its dependence on porosity and burnup. The different correlations for the fuel specific heat causes a maximum difference of 3%, and is not large enough to explain this temperature difference. A possible explanation is the difference in the radial power profile, which in FREY is flatter than in TU. This means that in FREY more heat is produced in the inner part of the fuel (Fig. 8).

8.6 Comparison of stresses in the cladding

During most of the calculation period, FREY predicted smaller stresses in the cladding than TU

FREY gave higher stresses than TU (as expected, due to the higher fuel radial expansion in FREY).

9 CONCLUSIONS

Coolant flow channel models were excluded from the code comparison by using common thermal boundary conditions. The differences between the code calculations were small. Clad inner temperatures and fuel rim temperatures were nearly identical. A possible explanation for the 40-50°C higher central temperatures predicted by FREY could be due to the flatter radial power profile in FREY (the correlation in TU for fuel thermal conductivity, and its dependence on porosity and burnup, was installed into FREY). The differences in the specific heat are too small to explain the temperature differences. However, it should be emphasised that a temperature difference of 40-50°C is negligible in fuel modelling calculations.

FREY calculated larger fuel axial elongation and radial expansion than TU. Consequently the stresses in the cladding were also larger in the FREY calculation. Neither FREY nor TU calculated fuel melting or clad failure.

REFERENCES

- [1] K. Lassmann, "TRANSURANUS: a fuel rod analysis code ready for use", Journal of Nuclear Materials, **188** (1992).
- [2] "FREY-01: Fuel Rod Evaluation System", EPRI NP-3277a, Volumes 1-4, Rev. 3 (1994).
- [3] H. Wallin, "High burnup structure: its characteristics, formation mechanisms and consequences in power excursions and RIA - literature review", PSI Internal Report, TM-43-01-14 (2002).
- [4] U.S. Nuclear Regulatory Commission, Proc. NRC 3rd PIRT Meeting, 1999
- [5] MATPRO-Vers. 11, "A handbook of material properties for use in the analysis of lightwater reactor fuel rod behaviour", NUREC/CR 0497 TREE 1280 (1979).
- [6] F. Lemoine, "High burnup fuel behaviour related to fission gas effects under reactivity initiated accidents (RIA) conditions", Journal of Nuclear Materials, **248**, 238-248 (1997).

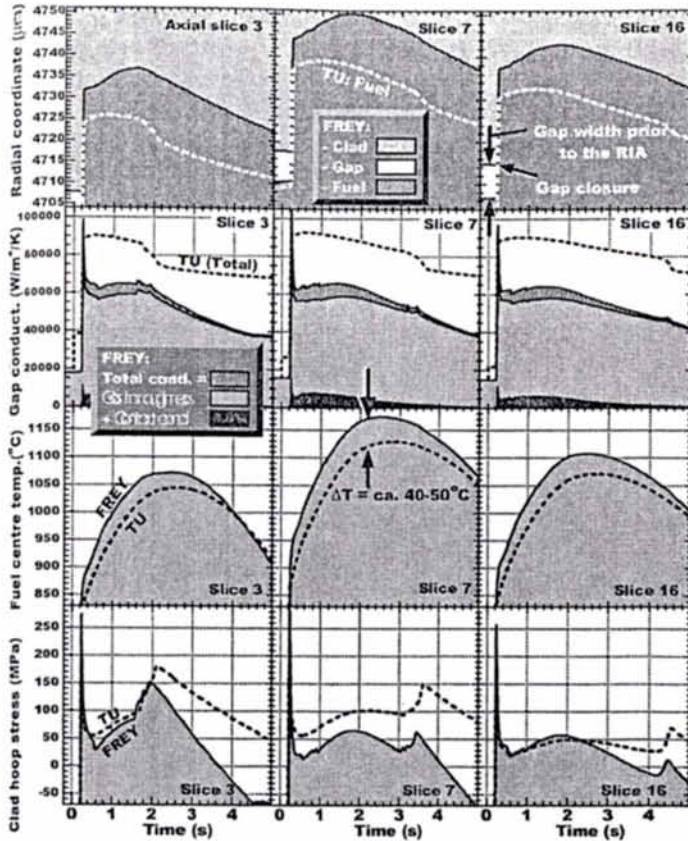


Fig. 9: Central variables (FREY vs. TU).

At the end of the DNB, the clad cools down more than the fuel and contracts against it, which explains the peaks in stress at the end of the calculation period.

8.7 Other results

Neither TU nor FREY have a valid model for burst release at high burnup. Consequently, only negligible fission gas release was calculated during the RIA. The inner gas pressure in the calculations reflects mainly the changes in rod free volume and gas temperature during the RIA (Table 3).

Neither code calculated failing of the clad.

Table 3: Some maximum values during the RIA (FREY vs. TRANSURANUS).

Parameter	TRANSURANUS results:			FREY results:		
	Max. value	Time (s)	Axial slice	Max. value	Time (s)	Axial slice
Fuel central temperature	1130°C	2.87	7	1174°C	2.56	7
Fuel rim temperature*	724°C	0.234	7	779°C	0.232	7
Fuel enthalpy	293 J/g	1.152	7			
Clad inner temperature	681°C	0.70	8	668°C	0.700	10
Pin inner pressure	8.75 MPa	1.74	-	7.27	1.00	-
Average equivalent stress in clad	196 MPa	0.238	5			
Clad hoop stress	178 MPa	0.238	4	287 MPa	0.232	5

* Refers only to the most outer fuel region. Temperature is notably higher slightly towards the fuel centre.